

Ab-Initio Calculation of the Metal-Insulator Transition in Lithium rings

Beate Paulus, Krzysztof Rosciszewski*, Peter Fulde

Max-Planck-Institut für Physik komplexer Systeme, Nöthnitzer Straße 38, D-01187 Dresden, Germany

** Institute of Physics, Jagellonian University, Reymonta 4, Pl 30-059 Krakow, Poland*

Hermann Stoll

Institut für Theoretische Chemie, Universität Stuttgart, D-70550 Stuttgart, Germany

We study how the Mott metal-insulator transition (MIT) is affected when we have to deal with electrons with different angular momentum quantum numbers. For that purpose we apply ab-initio quantum-chemical methods to lithium rings in order to investigate the analogue of a MIT. By changing the interatomic distance we analyse the character of the many-body wavefunction and discuss the importance of the $s-p$ orbital quasi-degeneracy within the metallic regime. The charge gap (ionization potential minus electron affinity) shows a minimum and the static electric dipole polarizability has a pronounced maximum at a lattice constant where the character of the wavefunction changes from significant p to essentially s -type. In addition, we examine rings with bond alternation in order to answer the question under which conditions a Peierls distortion occurs.

I. INTRODUCTION

When the lattice constant of a metallic system is sufficiently enlarged it will become an insulator, before eventually we end up with a collection of well separated atoms. This metal to insulator transition was first pointed out by Mott([1] and references therein) and has stimulated a tremendous amount of work for a better understanding of it. The standard model for these investigations has been the Hubbard Hamiltonian². It assumes one orbital per site and the electronic Coulomb interactions are reduced to an on-site Coulomb integral U . By applying different approximations Hubbard was able to quantify the conditions for the occurrence of a M-I phase transition. For that reason it is often called a Mott-Hubbard transition. More recently, the dynamical mean-field theory (DMFT) has been applied to the Hubbard Hamiltonian with one electron per site and has further elucidated details of the transition (for an overview and further references see, e.g., [3]).

The purpose of the present work is to go beyond the Hubbard model in order to understand better how other features might influence the transition in a realistic system. Lithium is a metal with a strong contribution of p electrons to the conduction band. With increasing lattice constant the ratio of p and s electrons is changing and in the atomic limit we are dealing with a pure $1s^2 2s$ atomic state. One of the questions we would like to have answered is the effect of low-energy atomic excitations from $2s$ to $2p$ on the M-I transition. In order to come

close to a realistic description of metallic systems we investigate a ring of Li atoms applying quantum-chemical methods for a treatment of electronic correlations.

In terms of a Hubbard model the Li-Li distance would correspond to the hopping term t . Instead of only an on-site Coulomb repulsion as in the Hubbard model we take here into account all possible Coulomb matrix elements. But in the limit of large separations of atoms only the on-site Coulomb repulsion remains.

The largest ring which we can treat at the multi-reference configuration-interaction (MRCI) level, without excessive computations, consists of 10 Li atoms. A medium-size basis set consisting of Gaussian type orbitals (GTO's) is used in the calculations. Usually the onset of insulating behaviour is characterized by the appearance of a gap. However, with a finite number of Li atoms in the ring we always have a finite energy difference between consecutive energy levels. Therefore, when the atomic distance is changed we must look for a change in the pattern between the highest occupied molecular orbital (HOMO) and the lowest unoccupied orbital (LUMO). These quantities are only accessible at the mean-field level. At the correlated level, we select three quantities which can give insight as regards the transition behaviour. MRCI methods can yield very good approximations to the exact ground-state wavefunction. The character of this wave function will be the first criterion. A second quantity which we calculate is the one-particle energy gap defined as the energy difference which is obtained if an electron is added to, or removed from the system. As a third quantity, we determine the static dipole polarizability of the system by applying a small homogeneous electric field. These three quantities are determined as functions of the nearest-neighbour Li-Li distance in the ring, and we discuss how the metal-insulator transition shows up in them. For these quasi-one-dimensional systems, the question arises whether we can gain energy by dimerization (Peierls distortion). We address this question by allowing for a bond alternation. In the next section we will discuss some technical details (Sect. II). In Sect. III, we present the results of different mean-field methods, for Li rings with increasing number of Li atoms and with increasing Li—Li distance. The behaviour of the many-body wavefunction is discussed in Sect. IV. Gap energies are presented in Sect. V and polarizabilities in Sect. VI. The Peierls distortion is considered in Sect. VII and conclusions follow in Sect. VIII.

Basis set	IP (a.u.)	EA (a.u.)	α (a.u.)	d_{dimer} (Å)
aug-cc-pVDZ	0.196	0.0151	166.0	2.73
aug-cc-pVTZ	0.196	0.0176	167.2	2.69
aug-cc-pVQZ	0.196	0.0209	167.5	2.68
[4s]	0.196	0.0019	0.000	3.03
[3s1p]	0.196	0.0150	164.8	2.85
[4s1p]	0.196	0.0212	165.6	2.85
[4s2p]	0.196	0.0216	165.6	2.73
[5s2p]	0.196	0.0218	166.6	2.67
exp.	0.198 ²⁷	0.0227 ²⁷	164.8 ¹³	2.67 ²⁷

TABLE I. ACPF values of the ionization potential (IP), the electron affinity (EA), and the dipole polarizability (α) of the Li atom are listed for different basis sets. Corresponding values for the bond length (d_{dimer}) of the Li₂ molecule are listed, too.

II. TECHNICAL DETAILS

The application of quantum-chemical *ab-initio* methods to Li rings is at the focus of the present work. Starting from a mean-field Hartree-Fock (HF) description, we re-optimize the valence wavefunction in multi-configuration self-consistent-field (MCSCF) calculations, keeping the 1s core electrons frozen at the HF level. Thereby, the number of valence active-space orbitals is chosen equal to (or larger than) the number of Li atoms of the system, and all possible occupations of these orbitals are accounted for. With this choice, we can properly describe the dissociation limit where each atom has one valence electron. On top of the MCSCF calculations, we apply the multi-reference averaged coupled pair functional (MRACPF) method^{5,6}. Here, all configuration-state functions are included which can be generated from the MCSCF reference wavefunction by means of single and double excitations from the active orbitals. These calculations are performed with the program package MOLPRO⁹⁻¹¹.

The GTO one-particle basis set used for the MCSCF/MRACPF calculations of the present work is derived from the correlation-consistent polarized valence double-zeta (cc-pVDZ) basis set of Dunning and co-workers¹². From this set, we select the three *s* functions and the first contracted *p*-function. To describe the negatively charged system, we add an even-tempered diffuse *s*-function (exponential parameter: 0.0107) resulting in a [4s1p] basis set. We checked the quality of this basis by calculating the electron affinity (EA), the ionization potential (IP) and the dipole polarizability of the Li atom (Table I). The *p* function is essential to describe the EA and the polarizability properly. Whereas the IP is weakly dependent on the size of the basis set used, because correlation effects are absent (core-valence correlation is neglected), the EA substantially increases when a diffuse *s*-function is added. A second diffuse *s*-function or a diffuse *p*-function have nearly no influence. The polarizability only slightly depends on the basis-set quality

$a = a_0$	EA	IP
HF	0.0208	0.1554
MCSCF	-0.0027	0.1672
ACPF	0.0335	0.1812
FCI	0.0321	0.1820
$a = 1.5a_0$	EA	IP
ACPF	0.0539	0.1530
FCI	0.0500	0.1548
$a = 2.0a_0$	EA	IP
ACPF	0.0448	0.1703
FCI	0.0409	0.1707

TABLE II. The EA and IP of Li₆ are listed for different levels of approximations and different Li-Li distances.

beyond cc-pVDZ, if the basis set contains at least one *p* function. The errors of the selected [4s1p] basis set as compared with experimental data are 1% for the IP, 7% for the EA and 0.5% for the polarizability. Thus, the [4s1p] basis although being relatively small can describe with sufficient accuracy all quantities we are interested in and is taken as default basis set in the subsequent calculations.

The Li—Li distance in 3-dimensional Li metal is $a_0=3.03\text{\AA}$ ⁴, while the equilibrium distance of the Li₂ dimer (2.67Å²⁷) is smaller by about 10%. For the Li₁₀ ring, we calculate an equilibrium distance of 3.06Å which is very similar to the bulk nearest-neighbour distance. Note, however that the [4s1p] basis overestimates the Li₂ bond length by 0.18 Å (the lack of a second *p* function is mainly responsible for this error, cf. Table I); if this bond-length error carries over to Li₁₀, we would have an equilibrium distance of around 2.9 Å for this system.

III. MEAN-FIELD DESCRIPTION

As a first step of our MIT study for Li rings, we performed mean-field (Hartree-Fock and density-functional (DFT)) calculations for various ring lengths and internuclear distances. With the Crystal program¹⁴ we can do HF calculations for the one-dimensional infinite Li chain. As basis set we selected the optimized [3s2p] basis set for the three-dimensional metal¹⁵. In Fig.1, the Hartree-Fock (HF) band structure is shown for the bulk equilibrium internuclear distance a_0 , and for $a = 2.5a_0$ which corresponds to the dissociation limit. In both cases the Fermi energy lies within the 2s band, but the band width is significantly reduced with increasing Li—Li distance. The predominant 2p band is very flat near the dissociation limit and well separated from the 2s band, whereas for a distance a_0 there is no gap between the 2s and 2p band.

For finite systems we applied the Turbomole *ab-initio* program package¹⁶ to obtain mean-field results for very long rings up to $n = 170$. We explicitly imposed spatial-symmetry restrictions on our closed-shell wavefunctions

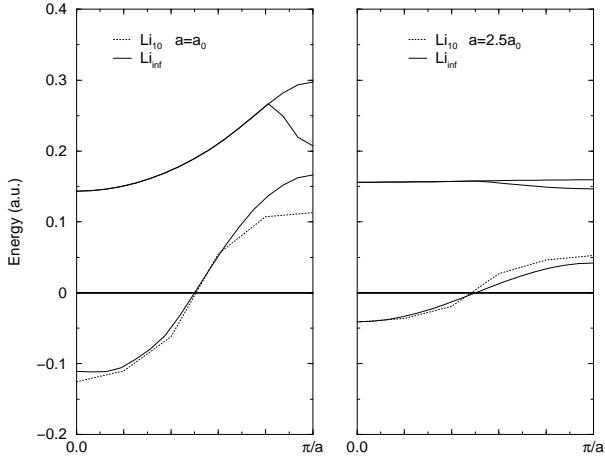


FIG. 1. Hartree-Fock band structure for the infinite Li chain for two different Li—Li distances. The Fermi energy is set to zero. In addition, a band structure obtained from the levels of Li_{10} is plotted (dashed curve); for comparison, the center of the $2s$ band is shifted to zero.

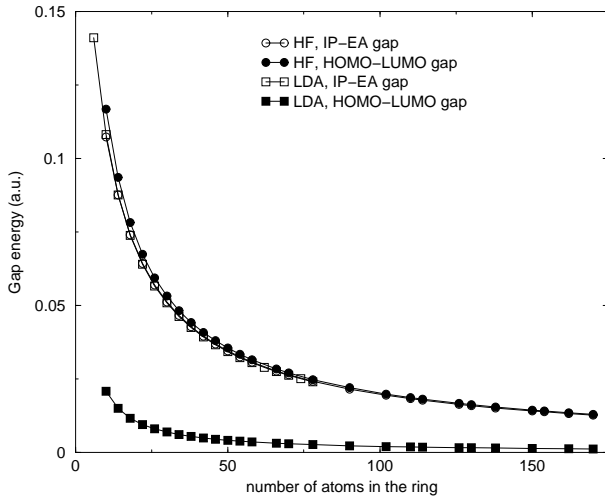


FIG. 2. Mean-field results (HF and LDA) for finite Li rings, in dependence of the number of atoms in the ring. The Li—Li distance is fixed at the metallic value ($a = a_0$).

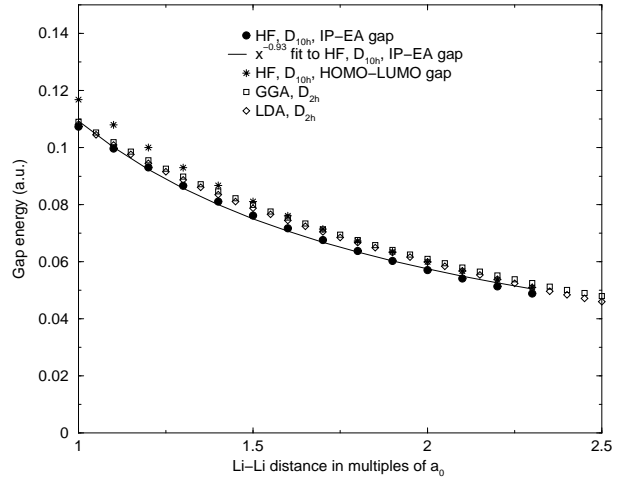


FIG. 3. Mean-field results (HF in D_{10h} symmetry, DFT(LDA and GGA) in D_{2h} symmetry) for a Li_{10} ring, in dependence of the Li—Li distance. The gap energy is taken as the difference of IP and EA; in the HF case, also the HOMO-LUMO gap value is given.

in order to avoid symmetry breaking. (For rings with $n > 30$, the HF approximation favours a symmetry broken ground state.) If we generate a HF band structure from the orbital energies of a Li_{10} ring and shift the Fermi energy to zero (dashed curve in Fig.1), the band width and band shape correspond well to that of the infinite chain, for both $a = a_0$ and $a = 2.5a_0$.

The energy gap of Li rings with different number of atoms, at a fixed Li—Li distance of $a = a_0$, is shown in Fig. 2. In a mean-field approach, the gap energy can either be calculated as HOMO-LUMO gap in the neutral system or by adding and subtracting an electron to the system, i.e., as difference of the IP and EA. At the HF level both approaches (approximately) coincide according to Koopmans' theorem¹⁷. Slight differences occur for smaller rings due to relaxation of the orbitals when the electron number is changed. This effect is missing in the HOMO-LUMO gap. Calculating the IP-EA gap with density functional theory in the local-density approximation (LDA)¹⁸, the results coincide well with the HF results. Note that in LDA the HOMO-LUMO gap is much smaller. This gap is directly related to an excitation energy other than the IP-EA gap. The decay of the IP-EA gap with increasing number of atoms in the ring is slow ($n^{-0.76}$). (If we would regard the finite ring as consisting of free electrons in a box, the decay should be proportional to $(\text{box-length})^{-1}$.) Despite the slow closing of the gap, even for Li_{10} it lies well within the band width of the infinite chain.

For the Li_{10} ring, we also calculated the behaviour of the IP-EA gap with increasing Li—Li distance, from a_0 to $2.5a_0$ (Fig.3). For the mean-field approaches, HF and DFT (both LDA¹⁸ and GGA^{19,20}), the gap is

monotonously closing. Thereby, the differences between the DFT variants and the differences between DFT and HF are not larger than that between the HOMO-LUMO and IP-EA values at the HF level. (Small differences may also arise due to the use of different formal symmetries (D_{2h} for DFT, D_{10h} for HF).) If we would model the ring by free electrons in a box again, the decay of the HOMO-LUMO gap should be proportional to $(\text{box-length})^{-2}$. This is in contrast to an approximate a^{-1} decrease obtained in our mean-field calculations, which shows that the electrons are far away from the free-electron limit. It should be kept in mind, however, that the correct dissociation limit cannot be described with these methods, anyway. Only multi-configuration methods can properly describe both the dissociation limit and the metallic behaviour. Such calculations form the main part of our present work and will be discussed below.

IV. THE CHARACTERISTIC FEATURES OF THE GROUND-STATE WAVEFUNCTION

Taking the example of the Li_{10} ring, we want to study how the character of the many-body ground-state wavefunction changes when enlarging the Li—Li distance from $a = a_0$ to $a = 2.5a_0$. For that purpose we performed a MCSCF calculation^{7,8} for the lowest singlet state, on top of a closed-shell HF calculation like that described in the previous section. (Using the MOLPRO package, we had to formally change to D_{2h} symmetry, however.) The selection of the active space is a decisive step: It is well known that for a correct description of the dissociation limit in Li_{10} ten atomic $2s$ orbitals are needed, but for the metallic regime ($a \approx a_0$) it is not clear how many orbitals are really important. Therefore we performed a pilot MCSCF calculation for $a = a_0$ with a high number of active orbitals and selected those natural orbitals whose occupancies were above a certain threshold. Retaining orbitals with occupancies larger than 0.18 and rejecting all the others which have occupancies smaller than 0.03 resulted in 10 active orbitals, too. However, only the 9 energetically lowest ones fall into the same irreducible representations (in D_{2h} symmetry) as the 9 lowest-lying orbitals of the insulating regime, while the highest natural orbital of the metallic and insulating regime differ in symmetry. Therefore, we selected for our final MCSCF calculation a new set of 11 active orbitals which was generated as the union of the two sets of orbitals described above. These orbitals were reoptimized at the MCSCF level. Finally, we performed a MRACPF calculation^{5,6} on top of the MCSCF, in order to include dynamical correlation effects as fully as possible. Note that the multi-reference treatment is important in both limits: in the metallic regime to describe static correlation with the quasi-degenerate $2p$ orbitals, and in the insulating regime to get the dissociation into degenerate $2s$ orbitals right.

Although we included in the active space all orbitals

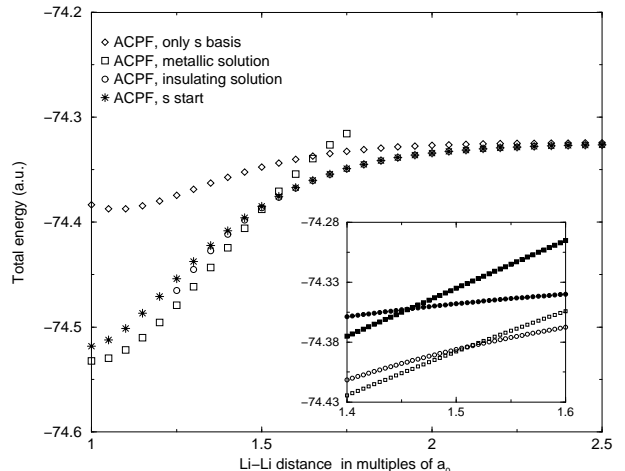


FIG. 4. MRACPF energies of the Li_{10} ring versus the Li—Li distance. The curves labeled “insulating wavefunction” and “metallic wavefunction” refer to different MCSCF zeroth-order wavefunctions used as reference for the subsequent MRACPF, cf. text. In the inset an enlarged part of the transition region is shown. The filled symbols correspond to the MCSCF values. The curves labeled “s start” and “only s basis” refer to calculations leaving out p functions in the MCSCF zeroth-order wavefunctions and at both the MCSCF and MPACPF levels, respectively.

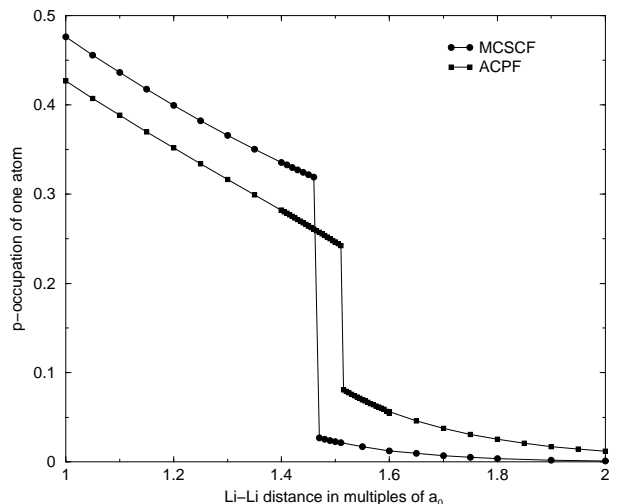


FIG. 5. The p occupation of the Li atom in a Li_{10} ring versus the Li—Li distance. The p occupations are calculated with the Mulliken population analysis.

which are important in the limits of small and large atomic distances, the total energy as function of the Li—Li distance is not a smooth curve (Fig. 4). This is so because the nature of the active orbitals changes along the curve. When starting the calculations from large a (wavefunction for the insulating state) and always using the previous solution as starting point for the next smaller lattice constant, this yields a slightly different solution in the region of the MIT than when starting from the metallic regime and increasing a . The difference is larger, of course, for the MCSCF energies than at the MRACPF level; With a full CI (i.e., including all higher excitations) the differences would vanish. However, a single smooth curve can be obtained even at the MRACPF level if it is based on a MCSCF calculation with only s functions in the active space. In that case p excitations appear at the MRACPF level only. It is clear that such a procedure favours the insulating solution: it yields a ground state energy for $a = a_0$ which is by ~ 0.02 a.u. higher than the value obtained with variationally optimized MCSCF orbitals. Still, the so obtained ground-state potential curve is qualitatively correct also in the metallic regime. It is interesting to compare it with a MRACPF curve obtained by leaving out p functions in the one-particle basis set altogether. Here, we still observe a (shallow) minimum near $a = a_0$, but the energy is higher by more than 0.1 a.u. Thus, p contributions amount to about two thirds of the binding energy of the Li_{10} ring.

Turning back now to our most accurate potential curve: The change of the character of the MRACPF wavefunction as well as that of the underlying MCSCF wave function as a function of a is seen best by a Mulliken population analysis for the p orbitals (Fig. 5). For the "metallic" MCSCF solution the atomic p orbital occupancy is nearly 0.5 at $a = a_0$ and slowly drops to 0.3 at $a \approx 1.5a_0$, while for the "insulating" solution it is less than 0.03 for $a \geq 1.5a_0$. Even in the MRACPF case, the p population changes by a factor of ~ 3 . Taking this rather dramatic change as a signature of the MIT we find for all investigated rings a region around $1.5a_0$, where the character of the wavefunction changes significantly.

V. THE ONE-PARTICLE ENERGY GAP

The energy gap of an insulator is determined by the energy differences between the ground state of the neutral system and the ones with one electron added and subtracted. In the case of a Li ring, we calculate the MRACPF ground-state energies of the Li_n^- , Li_n and Li_n^+ systems and determine $\text{EA} = E(\text{Li}_n^-) - E(\text{Li}_n)$ and $\text{IP} = E(\text{Li}_n^+) - E(\text{Li}_n)$ and from $\text{IP} - \text{EA}$ the corresponding gap. For a metallic solid adding and removing an electron cost an energy given by the chemical potential. In finite systems, there always remains the difference between the one-particle energies of the additional and the

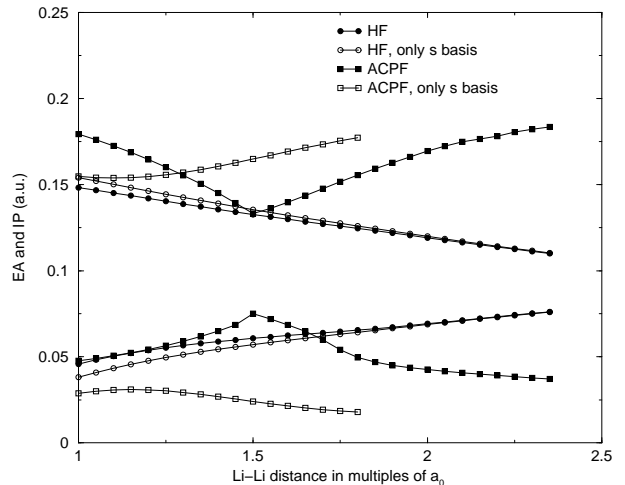


FIG. 6. HF and MRACPF values for the EA and IP of a Li_{10} ring, versus the Li-Li distance. For comparison, we add results from calculations without p functions in the basis set ("only s basis").

missing electron as well as the influence of relaxation and correlation effects.

The EA and IP for Li_{10} are plotted in Fig. 6. In the metallic regime, the HOMO-LUMO gap is expected to decrease with increasing Li-Li distance exactly like it happens for free electrons in a box with changing length.

In fact, at the HF level we obtain a monotonous shrinking of the gap, both with our standard basis set ($[4s1p]$) and with a pure s basis set ($[4s]$). The availability of p polarization functions stabilizes the charged systems as compared to the neutral one, leading to a slightly smaller gap for $a = a_0$ than with a pure s basis, but the difference goes to zero for $a \rightarrow \infty$ and the general trend of a closing gap with enlarging Li-Li nearest-neighbour distance is the same in both cases. However, the trend completely changes when correlation effects are included. The most important change concerns the $a \rightarrow \infty$ limit, where HF fails to describe correctly the dissociation. Instead of a closing of the gap, the correct limit is the difference between the atomic IP and EA. This limit is obtained indeed, in our MRACPF calculations. As already noted in Sect. 2, the atomic EA is severely underestimated in the case of a pure s basis set, but this is efficiently remedied with our standard $[4s1p]$ basis set. We furthermore note that the EA converges much slower to the atomic limit than IP ($\text{EA}(a = 2.35a_0) = 1.6$ EA(atom), $\text{IP}(a = 2.35a_0) = 0.94$ IP(atom)). We think that this is due to the larger size of the Li^- ion than of the Li^+ ion. Interestingly, the variation of IP and EA from $a = a_0$ to $a \rightarrow \infty$ is not completely monotonous. Already for the case of a pure s basis, the gap is nearly constant (and even slightly decreases) in the range $a_0 < a < 1.3a_0$, and only then gradually opens up to the atomic limit. In-

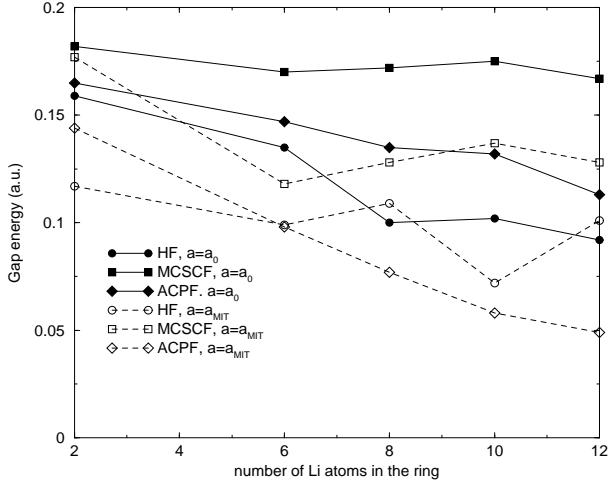


FIG. 7. HF, MCSCF and MRACPF one particle energy gaps are plotted versus the number of Li atoms in the ring for two different lattice constants, cf. text.

cluding p contributions leads to a significant increase of IP and EA for $a = a_0$ as well as to a distinctly non-monotonous behaviour of the gap as a function of a , with a minimum around $a = 1.5a_0$. The effect is due to a stabilization of the charged systems, with respect to the neutral one, by means of polarization clouds around holes/electrons. Thus, for a finite ring in the metallic regime the gap is closing when enlarging the lattice constant, at the MIT point it is minimal, then it starts to increase gradually approaching the atomic limit value.

We investigated the gap behaviour not only for the Li_{10} ring, but also for the Li_2 dimer, for the Li_6 and Li_8 rings, and for the Li_8 cube. (Li_4 arranged in a square has a negative EA; hence, the calculation of the one-particle energy gap does not make any sense. Li rings with odd number of Li atoms do not have a closed shell HF ground state and therefore are not considered here.) For Li_{12} , we performed calculations at $a = a_0$ and $a = a_{\text{MIT}}^*$, where a_{MIT}^* is defined as the point where the character of the MCSCF wavefunction changes from significant p character to an essentially s one. For all investigated ring systems, the minimal value of the gap occurs for nearly the same lattice constant in different rings (between $1.42a_0$ and $1.55a_0$). This distance coincides approximately with the one where the character of the wavefunction changes. In Fig.7 the energy gap at $a = a_0$ and $a = a_{\text{MIT}}^*$ is listed for different methods and for different ring lengths. When increasing the number of atoms in the ring, the minimal gap energy at the ACPF level decreases faster than the gap at $a = a_0$. Unfortunately, the behaviour of the gap for much longer rings cannot be calculated by the methods we use because it is computationally too expensive. The gap calculated at the MCSCF level seems to saturate for longer rings, i.e. only the dynamical correlations

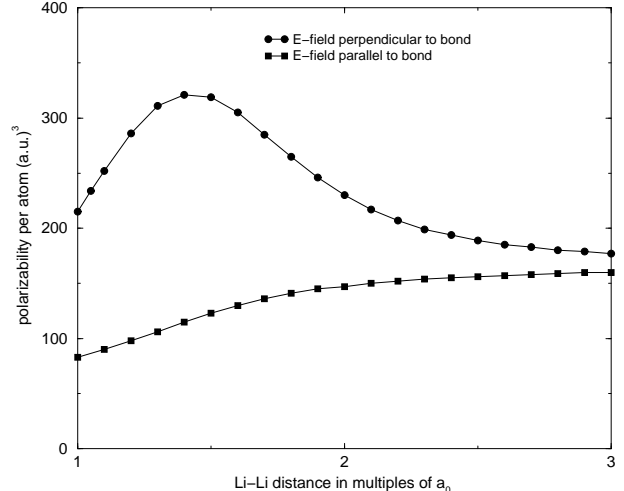


FIG. 8. The MRACPF static dipole polarizability of the Li_2 dimer, for the electric field parallel and perpendicular to the bond direction, is plotted versus the Li—Li distance.

are closing the gap. As yet, we cannot make a reasonable extrapolation and find out for which ring length a zero gap is to be expected. But for all investigated rings we found similar behaviour with increasing Li-Li distance independent of the number of Li atoms in the ring. In spite of this we reemphasize that although we have a finite system instead of a real metallic system, we still see a transition from a metallic-like regime (where the gap is closing with increasing Li-Li distance) to an insulating regime where the gap is opening towards the atomic limit.

In order to validate the methods used in the present paper, we performed full-CI (FCI) calculations²² for Li_6 at three different lattice constants, i.e., we determined the lowest variational energies in each case which can be obtained with our standard $[4s1p]$ one-particle basis set. The resulting EA and IP are listed in Table II. The ACPF values coincide well with the FCI results and therefore are expected to provide a reliable, quantitative description of the gap energy.

Finally, let us note, that we observe a similar minimal gap for the Li_8 cube, where no sharp jump in the p occupation pattern of the wave function is visible. In the cube, the minimal gap occurs at a somewhat larger distance ($1.65a_0$) than it does in the ring and is also a little bit larger (0.09 a.u.), but the qualitative behaviour remains the same.

VI. DIPOLE POLARIZABILITY

As a third quantity which can be used to define the MIT, we calculate the static electric dipole polarizability of the system. We apply a static electric field of strength

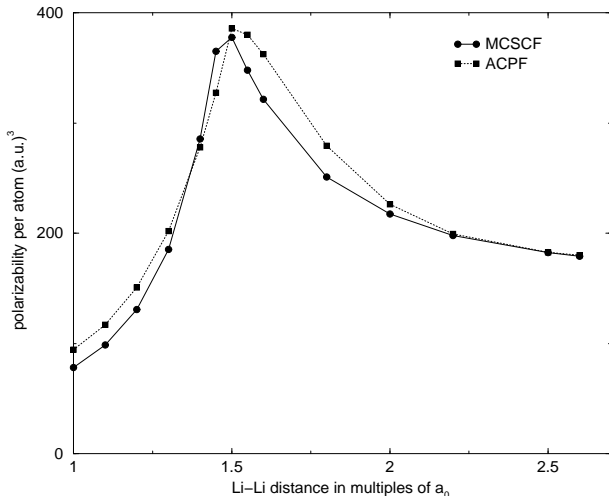


FIG. 9. The static dipole polarizability of the Li_{10} ring, for the electric field in the ring plane, is plotted versus the Li—Li distance for two different methods.

up to 0.035 a.u. and perform a quadratic fit for the energy of the system, $E(\mathcal{E}) = E(0) - \frac{1}{2}\alpha\mathcal{E}^2$, yielding the polarizability α . Higher order terms can be neglected for the small field strengths we chose. For a metallic system the polarizability should be infinite, therefore a steep increase of the polarizability can indicate an insulator-metal transition.

As a test example, we selected the Li_2 dimer and applied the \mathcal{E} field both in the bond direction and in a direction perpendicular to that, while gradually enlarging the Li—Li distance (Fig.8). At the equilibrium bond length, we obtain an average polarizability of 118 a.u. (the experimental value is 111 a.u.²⁴). If the electric is parallel to the bond direction, the polarizability exhibits a maximum at a Li—Li distance similar to that where the minimal gap occurs. For a field direction perpendicular to the bond, the polarizability increases monotonously to two times the atomic value as the HOMO-LUMO gap becomes smaller.

For the Li_{10} ring, we find the same behaviour as in the dimer when we apply the field perpendicular to the ring plane. When we apply the field in the ring plane we find a pronounced maximum. In Fig. 9, we plot the polarizability per atom for the Li_{10} ring, both at the MCSCF and MRACPF levels. A crossing of the curves occurs within the transition region, since we have two different solutions at the transition. MCSCF and MRACPF polarizability values differ only slightly. At $a = a_0$ the calculated MRACPF value is 94.4 a.u.. Experimental data are available for the static dipole polarizability of a Li_{10} cluster²³; unfortunately the cluster geometry is not fully known, but it can be supposed to be two- or three-dimensional. The experimental value is 70.2 a.u. and it roughly agrees with our value. As already noted, the

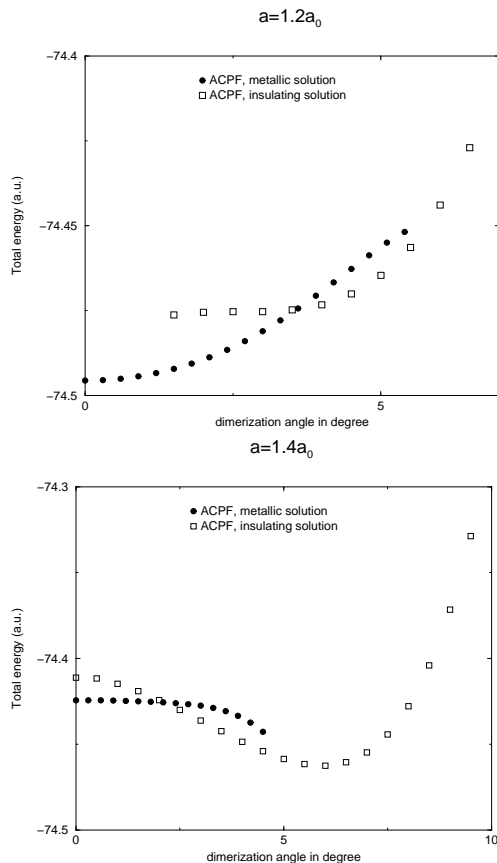


FIG. 10. The total energy of the Li_{10} ring is plotted versus the dimerization angle (defined as deviation from the ideal 36° angle in Li_{10} , in degree) for different average lattice constants.

polarizability increases with decreasing lattice constant (i.e., when coming from the insulating side). For an infinite system the polarizability should diverge at the MIT. We see a precursor of this divergence and can therefore use it to define a MIT even for a finite system. The rapid decay of the polarizability in both the metallic and the insulating regime is due to the opening of the gap.

VII. LATTICE DISTORTION

In this last section, we allow for a bond alternation along the ring, so that the Li atoms can form dimers. For average lattice constants larger than that where the M-I transition occurs (i.e., for lattice constants where the insulating solution is the ground state) the formation of dimers is energetically favoured. The resulting dimer internuclear distance agrees well with the calculated distance of the free dimer (2.88 Å). The energy gain is due to bond formation between two Li atoms. In the metallic regime ($a \leq a_{\text{MIT}}$) a Peierls distortion²⁵ occurs, stabilizing the dimerized state (see Fig 10). However, decreasing the lattice constant further, we found a point ($a = 1.3a_0$ for Li_{10}), below which the equidistant arrangement is the ground state, which would imply a metallic state for the

infinite chain.

At the HF level, a bond alternation is found for all (average) lattice constants; electronic correlations seem to suppress this bond alternation at the equilibrium lattice constant. This is in contrast to poly-acetylene, where correlations reduce the bond alternation without fully suppressing it²⁶.

VIII. CONCLUSIONS

We investigated the analogue of the metal-insulator transition for one-dimensional lithium, applying high-level quantum-chemical *ab-initio* methods. The aim of this investigation was to find out how the MIT is modified from the one in the Hubbard model, when we have to deal with several orbitals per site. We have chosen Li as an example since here the different orbitals correspond to different angular momentum quantum numbers, i.e., s and p electrons. By treating a Li_{10} ring we could apply accurate quantum-chemical *ab initio* methods. Following the original ideas of Mott, a metallic system will become an insulator when the lattice constant is sufficiently large. But in distinction to the Hubbard model it is here the interplay of the s and p orbitals which strongly affects the MIT. At the transition point ($a_{\text{MIT}} \approx 1.5a_0$) the character of the many-body wavefunction changes from significant p to essentially s character. Therefore it must be kept in mind that in a real solid the re-population of orbitals belonging to different angular momenta may have similarly strong influence on the MIT as changes in the ratio of the Hubbard U to the kinetic energy. We found that approximately at the same interatomic distance where the p character of the wavefunction changes so strongly, the one-particle energy gap is minimal and the static electric polarizability has a maximum. Increasing the ring length, the minimal gap closes faster than the gap at the equilibrium distance; the reduced level spacing for both longer rings and larger lattice constants enhances dynamical correlation effects. Allowing for a bond alternation in the ring, the system dimerizes for all (average) lattice constants larger than $\sim 1.3a_0$, for the insulating case due to Li_2 molecule formation, for the metallic case due to Peierls distortion. For even smaller lattice constants, the correlations stabilize the equidistant arrangement of the Li atoms along the ring. Further investigations are planned for open boundary conditions (i.e., linear fragments of the infinite chain) and for other alkali metals (thereby, e.g. mixing different alkali atoms to mimic the ionic Hubbard model).

APPENDIX A: LIST OF ABBREVIATIONS

MIT	metal-insulator transition
HOMO	highest occupied molecular orbital
LUMO	lowest unoccupied molecular orbital
GTO	Gaussian type orbital
cc-pVDZ	correlation consistent polarized valence double-zeta
HF	Hartree-Fock
MCSCF	multi-configuration self-consistent field approximation
MRCI	multi-reference configuration interaction
MRACPF	multi-reference averaged coupled pair functional
IP	ionization potential
EA	electron affinity
DFT	density functional theory
LDA	local density approximation
GGA	generalized gradient corrected approximation
FCI	full CI – configuration interaction with all excitations

-
- ¹ N.F. Mott, *Metal-Insulator Transition*, 2nd Edition, Taylor and Francis, London, 1990.
 - ² J. Hubbard, *Proc. Roy. Soc. London Ser. A* **276**, 238 (1963); *ibid* **277**, 237 (1963).
 - ³ F. Gebhard, *The Mott Metal-Insulator Transition*, Springer, Berlin (1997).
 - ⁴ C. Kittel, *Introduction to solid state physics*, Wiley, New York (1996) 7. ed.
 - ⁵ R.J. Gdanitz and R. Ahlrichs, *Chem. Phys. Lett.* **143**, 413 (1988).
 - ⁶ H.-J. Werner and P. J. Knowles, *Theor. Chim. Acta* **78** (1990) 175.
 - ⁷ H.-J. Werner and P. J. Knowles, *J. Chem. Phys.* **82** (1985) 5053.
 - ⁸ P. J. Knowles and H.-J. Werner, *Chem. Phys. Lett.* **115** (1985) 259.
 - ⁹ MOLPRO version 2002.6 - a package of *ab-initio* programs written by H.-J. Werner and P. J. Knowles with contributions from J. Almlöf, R. D. Amos, A. Bernhardsson, A. Berning, P. Celani, D.L. Cooper, M. J. O. Deegan, A.J. Dobbyn, F. Eckert, C. Hampel, G. Hetzer, T. Korona, R. Lindh, A.W. Lloyd, S.J. McNicholas, F.R. Manby, W. Meyer, M.E. Mura, A. Nicklass, P. Palmieri, R. Pitzer, G. Rauhut, M. Schütz, H. Stoll, A.J. Stone, R. Tarroni, and T. Thorsteinsson.
 - ¹⁰ P. J. Knowles and H.-J. Werner, *Chem. Phys. Lett.* **145** (1988) 514.
 - ¹¹ H.-J. Werner and P. J. Knowles, *J. Chem. Phys.* **89** (1988) 5803.
 - ¹² T. H. Dunning Jr., *J. Chem. Phys.* **90** (1989) 1007.
 - ¹³ W. D. Knight, K. Clemenger, W. A. de Heer and W. A. Saunders, *Phys. Rev. B* **31**, 2539 (1985).
 - ¹⁴ V.R. Saunders, R. Dovesi, C. Roetti, M. Causa, N. M. Harrison, R. Orlando, and C. M. Zicovich-Wilson, *Crystal 98 User's Manual*, Theoretical Chemistry Group, University of Torino (1998).

- ¹⁵ K. Doll, N. M. Harrison, and V. R. Saunders, *J. Phys.: Condens. Matter* **11**, 5007 (1999).
- ¹⁶ Turbomole Version 5 (2000) is designed by the Quantum Chemistry Group, University of Karlsruhe, Germany, by R. Ahlrichs, M. Bär, H.-P. Baron, R. Bauernschmitt, S. Böcker, M. Ehrig, K. Eichkorn, S. Elliott, F. Furche, F. Haase, M. Häser, H. Horn, C. Huber, U. Huniar, M. Kattannek, C. Kölmel, M. Kollwitz, K. May, C. Ochsenfeld, H. Öhm, A. Schäfer, U. Schneider, O. Treutler, M. von Armin, F. Weigend, P. Weis and H. Weiss; M. Häser and R. Ahlrichs, *J. Comput. Chem.* **10** (1989), 104; R. Ahlrichs, M. Bär, M. Häser, H. Horn and C. Kölmel, *Chem. Phys. Lett.* **162** (1989), 165.
- ¹⁷ T. A. Koopmans, *Physica* **1**, 104 (1933).
- ¹⁸ S.J. Vosko, L. Wilk and M. Nusair, *Can. J. Phys.* **58** (1980) 1200.
- ¹⁹ A.D. Becke, *Phys. Rev. A* **38** (1988) 3098.
- ²⁰ C. Lee, W. Yang, R.G. Parr, *Phys. Rev. B* **37** (1988) 785.
- ²¹ B. Paulus, *Chem. Phys. Lett.* **371**, 7 (2003).
- ²² P.J. Knowles and N.C. Handy, *Chem. Phys. Lett.* **111** (1984) 315.
- ²³ E. Benichou, R. Antoine, D. Rayane, B. Vezin, F.W. Dalby, Ph. Dugourd, and M. Broyer, *Phys. Rev. A* **59** R1 (1999).
- ²⁴ R. Antoine, D. Rayane, A.R. Allouche, M. Aubert-Frecon, E. Benichou, F.W. Dalby, Ph. Dugourd, M. Broyer and C. Guet, *J. Chem. Phys.* **110** (1999), 5568.
- ²⁵ R. E. Peierls, *Quantum Theory of Solids*, Clarendon, London (1955)
- ²⁶ G. König and G. Stollhoff, *Phys. Rev. Lett* **65**, 1239 (1990)
- ²⁷ A.A. Radzig and B.M. Smirnov, *Reference Data on Atoms, Molecules, and Ions*, Springer Series in Chemical Physics (ed. J.P. Toennies), vol. 31, Springer, Berlin (1985)